Supplementary Information

Room-temperature-persistent magnetic interaction between coordination complexes and nanoparticles in maghemite-based nanohybrids.

Leonardo Curti, Yoann Prado, Aude Michel, Delphine Talbot, Benoît Baptiste, Edwige Otero, Philippe Ohresser, Yves Journaux, Christophe Cartier-dit-Moulin, Vincent Dupuis, Benoit Fleury, Philippe Sainctavit, Marie-Anne Arrio,* Jérôme Fresnais* and Laurent Lisnard*
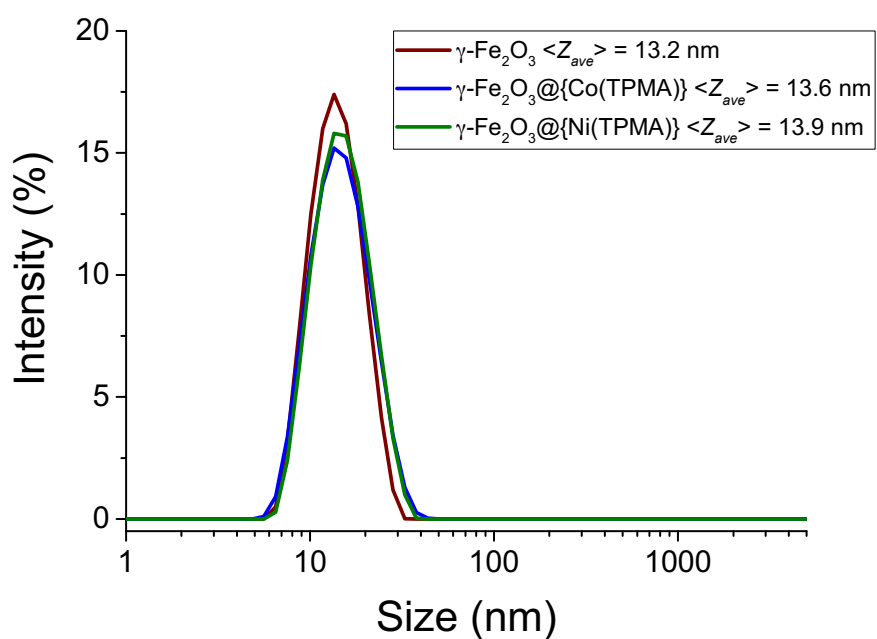
Figure S1. Intensity profiles of the DLS measurements for the as synthesized H_2O:MeOH 1:1 solutions of γ-Fe₂O₃, γ-Fe₂O₃@{Co(TPMA)} and γ-Fe₂O₃@{Ni(TPMA)} at 25°C.

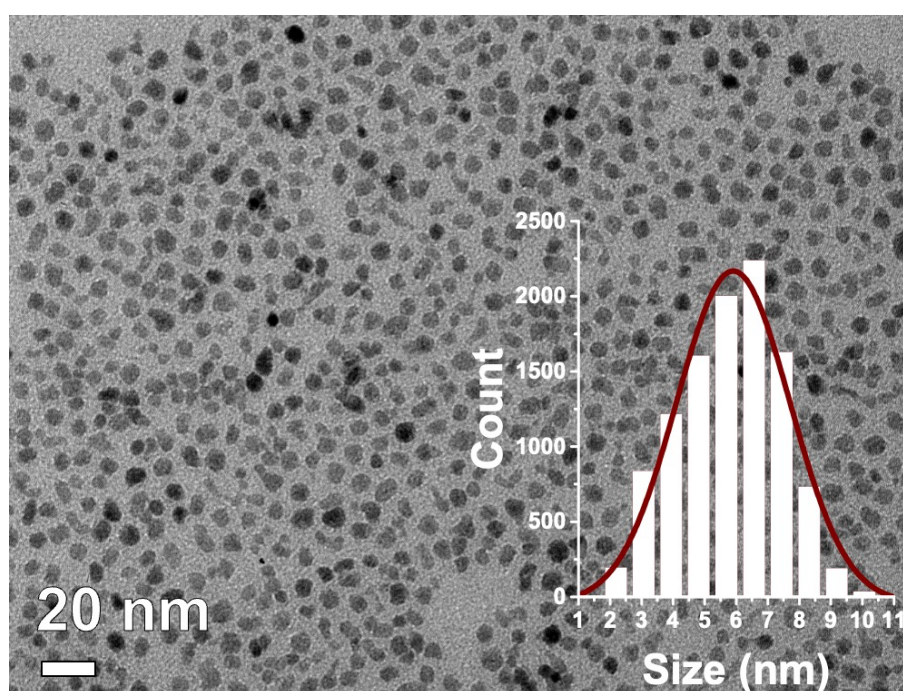**Figure S2.** TEM image and distribution profile of the γ-Fe₂O₃ nanoparticles (5.90 ± 1.8 nm).

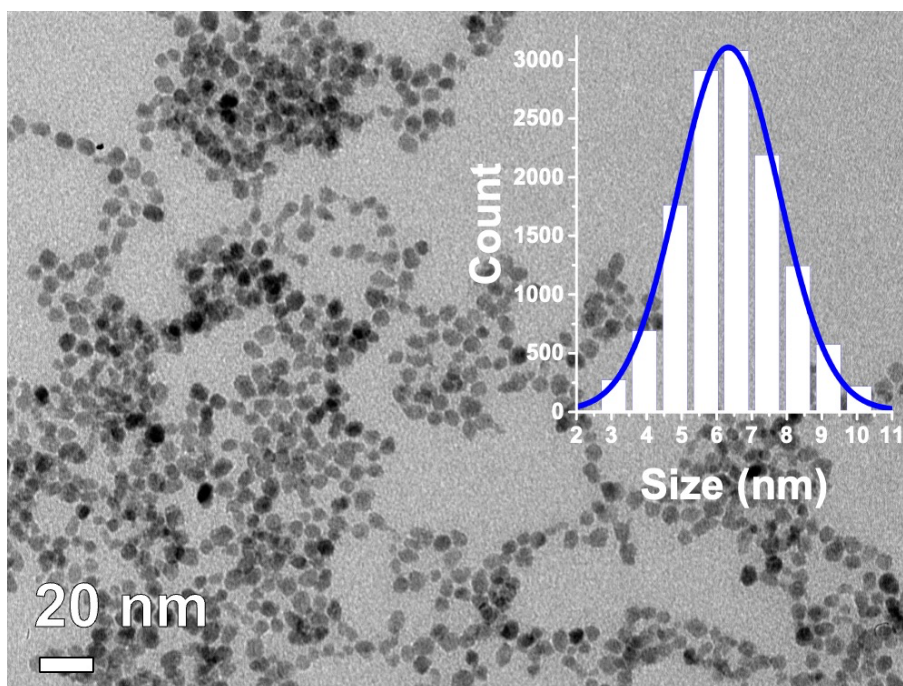**Figure S3.** TEM image and distribution profile of the γ-Fe$_2$O$_3$ nanoparticles functionalized with [Co(TPMA)Cl$_2$], **γ-Fe$_2$O$_3$@{Co(TPMA)}** (6.33 ± 1.4 nm).
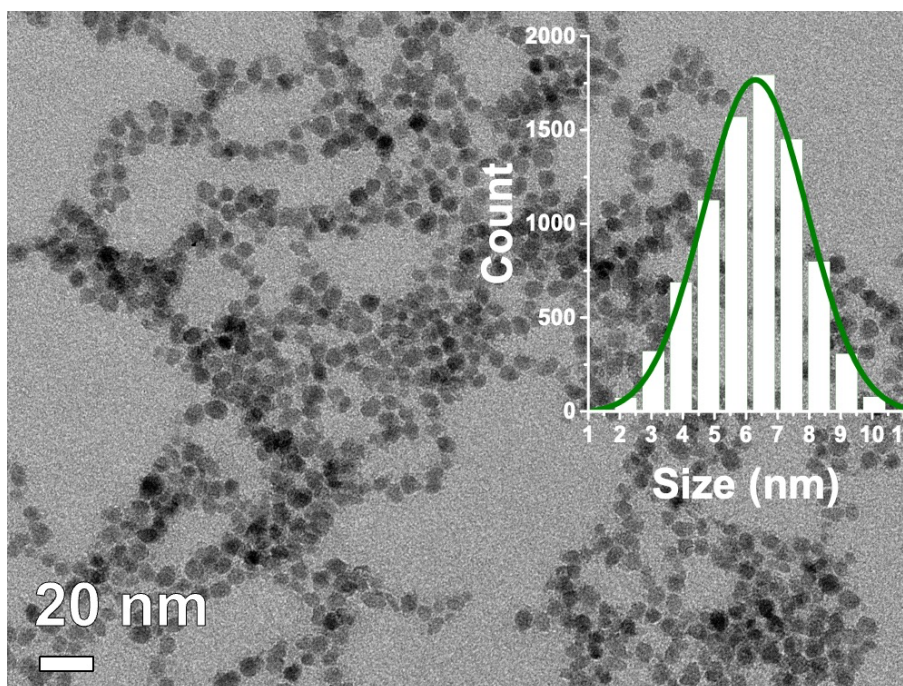
Figure S4. TEM image and distribution profile of the γ-Fe$_2$O$_3$ nanoparticles functionalized with [Ni(TPMA)Cl$_2$], **γ-Fe$_2$O$_3$@{Ni(TPMA)}** (6.33 ± 1.6 nm);
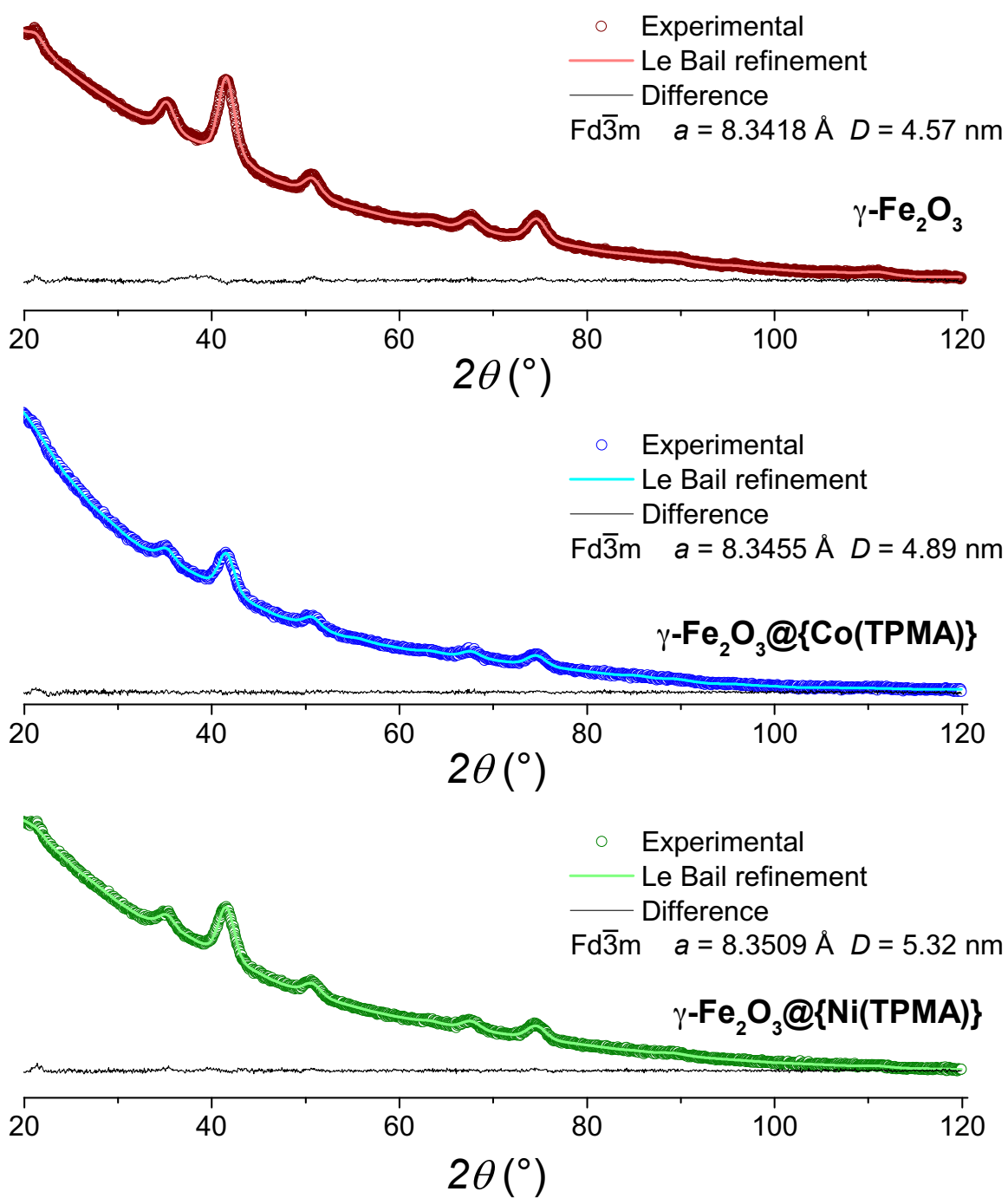
Figure S5. Powder X-ray diffraction patterns, Le Bail fit results and size determinations for compounds γ-Fe₂O₃, γ-Fe₂O₃@{Co(TPMA)} and γ-Fe₂O₃@{Ni(TPMA)}.
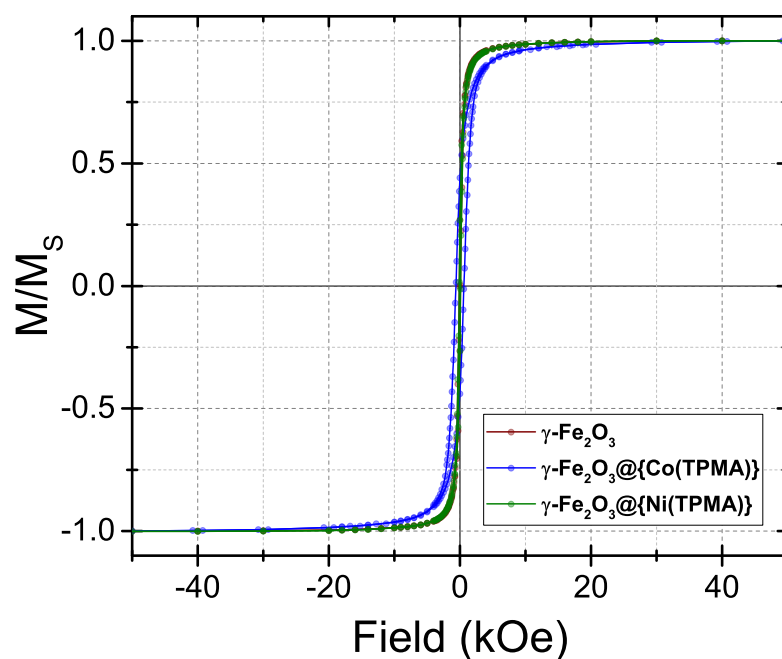
Figure S6. Field-dependence of the normalized magnetization for γ-Fe$_2$O$_3$, γ-Fe$_2$O$_3$@{Co(TPMA)} and γ-Fe$_2$O$_3$@{Ni(TPMA)} measured by SQUID at 5 K and in the ± 50 kOe range.
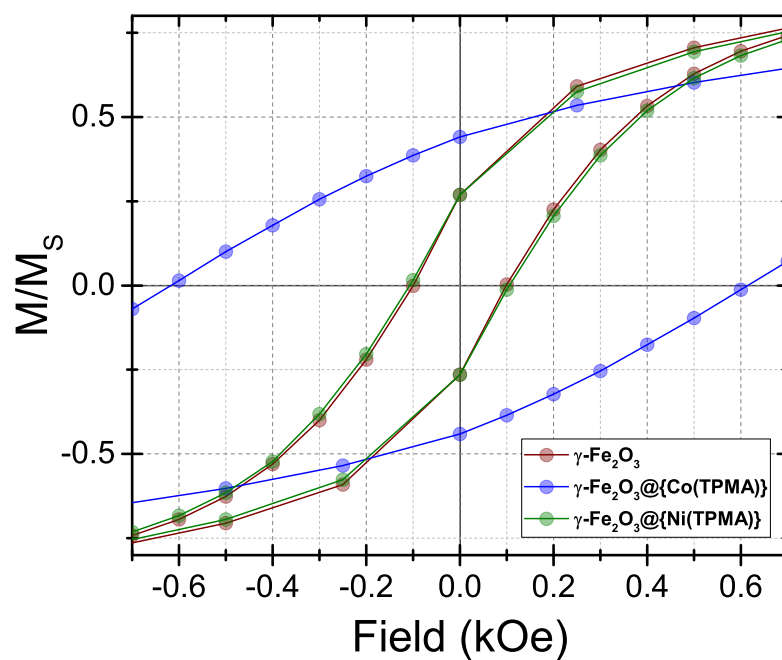

Figure S7. ± 700 Oe region of the field-dependence of the normalized magnetization for γ-Fe$_2$O$_3$, γ-Fe$_2$O$_3$@{Co(TPMA)} and γ-Fe$_2$O$_3$@{Ni(TPMA)} measured by SQUID at 5 K and in the ± 50 kOe range.
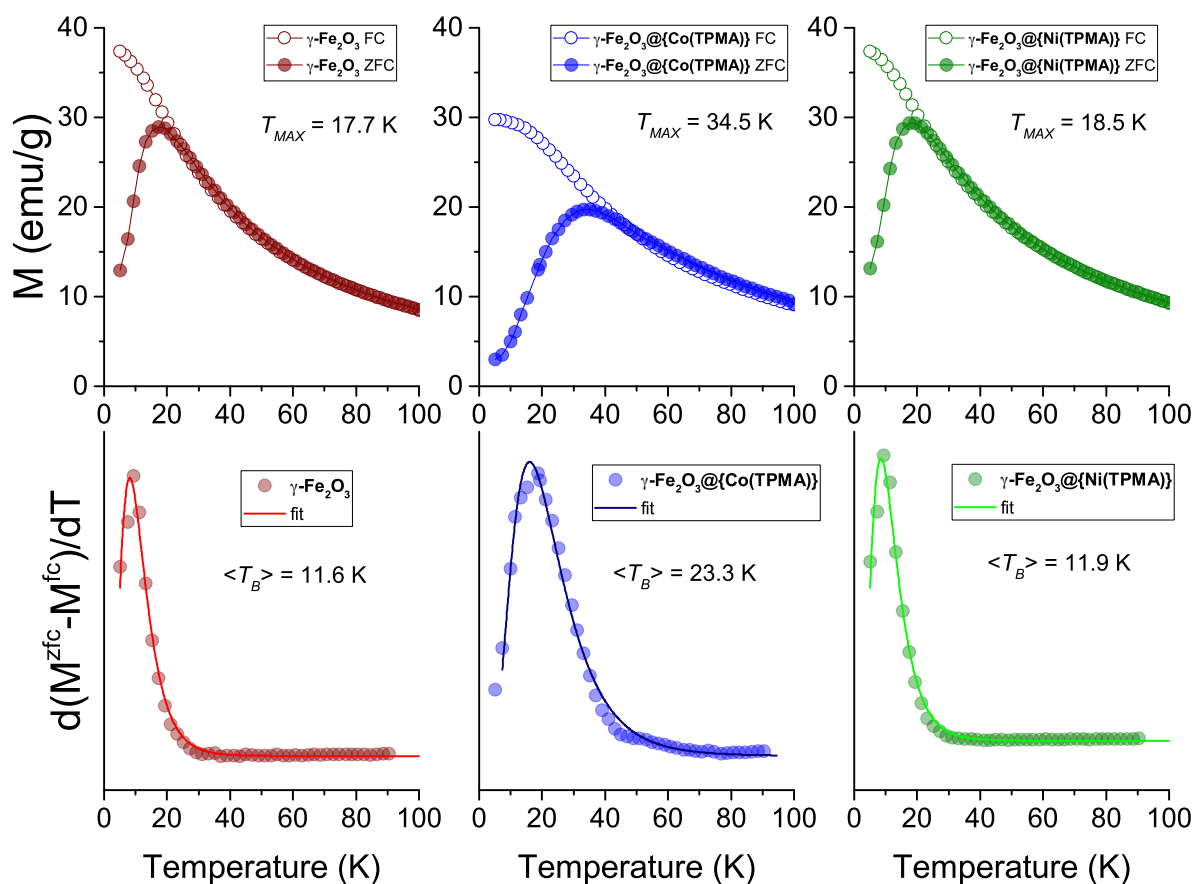
Figure S8. ZFC/FC curves measured by SQUID at 50 Oe between 5 and 100 K, with T_{MAX} values and fitting of $\langle T_B \rangle$ values for compounds **γ-Fe₂O₃**, **γ-Fe₂O₃@{Co(TPMA)}** and **γ-Fe₂O₃@{Ni(TPMA)}**.
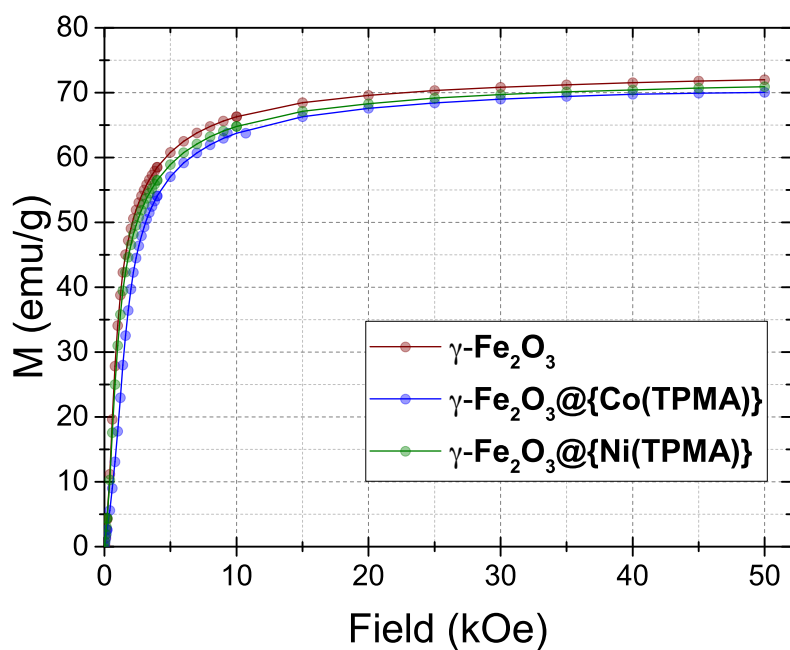
Figure S9. 1st magnetization curves measured by SQUID at 5 K from 0 to 50 kOe for **γ-Fe₂O₃**, **γ-Fe₂O₃@{Co(TPMA)}** and **γ-Fe₂O₃@{Ni(TPMA)}**.
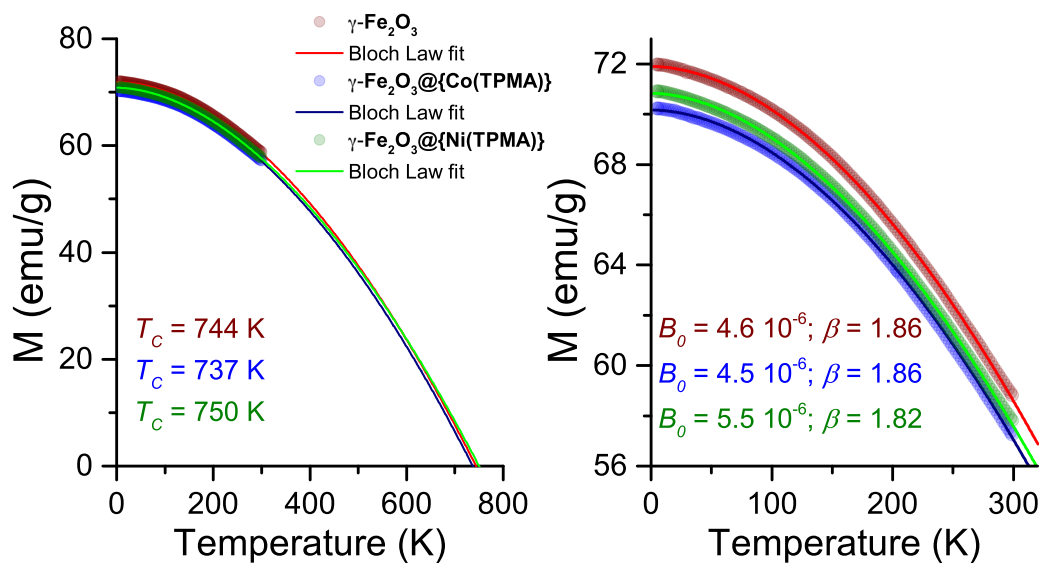
Figure S10. Temperature-dependence of the saturation magnetization measured by SQUID between 5 and 300 K at 50 kOe, with $M_S(T) = M_S(0)[1-B_0 T^{\beta}]$ Bloch Law fit parameters and T_C determination for compounds **γ-Fe₂O₃**, **γ-Fe₂O₃@{Co(TPMA)}** and **γ-Fe₂O₃@{Ni(TPMA)}**.
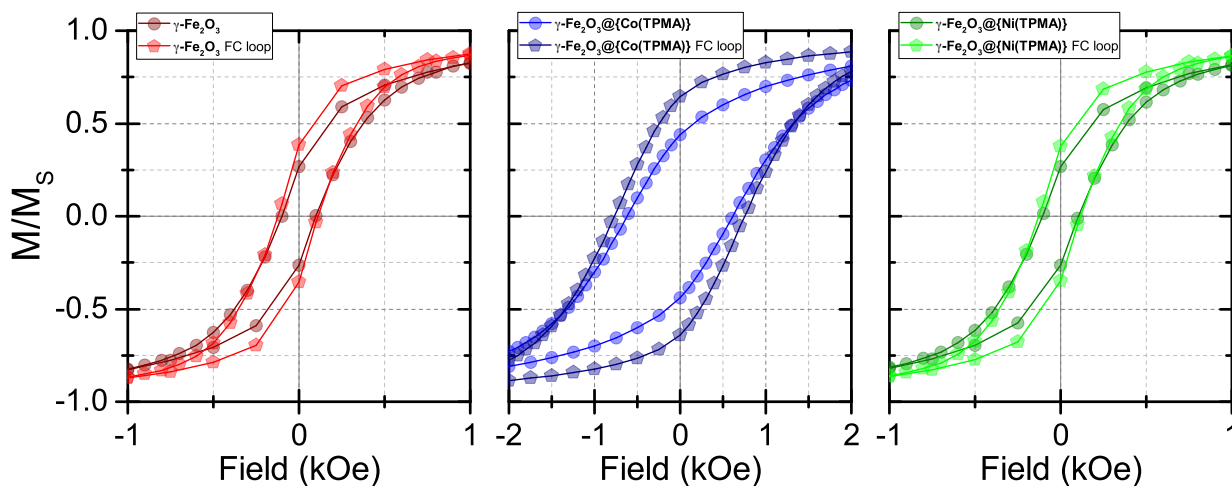
Figure S11. Hysteresis loops for **γ-Fe₂O₃**, **γ-Fe₂O₃@{Co(TPMA)}** and **γ-Fe₂O₃@{Ni(TPMA)}** measured by SQUID at 5 K and in the ± 50 kOe range and after a FC procedure at 50 kOe from 250 to 5 K.

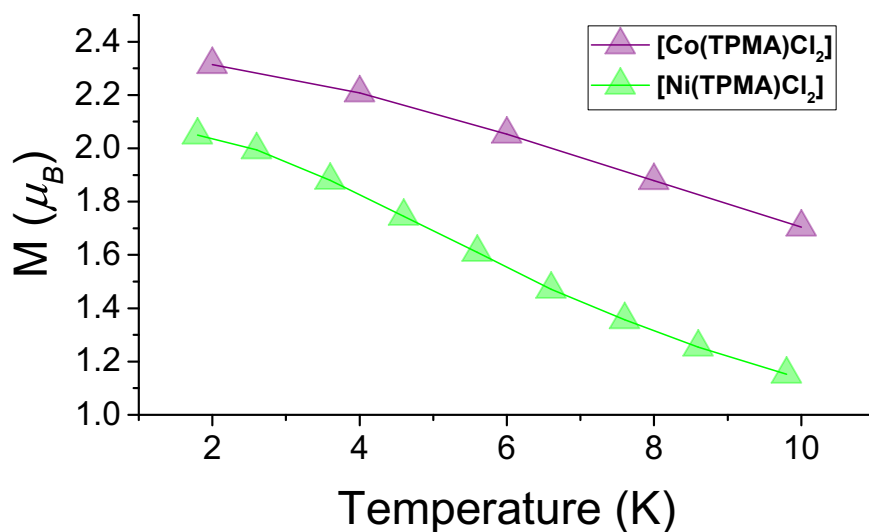**Figure S12**. Low temperature magnetization curves for [Co(TPMA)Cl₂] and [Ni(TPMA)Cl₂] measured by SQUID at 60 kOe.
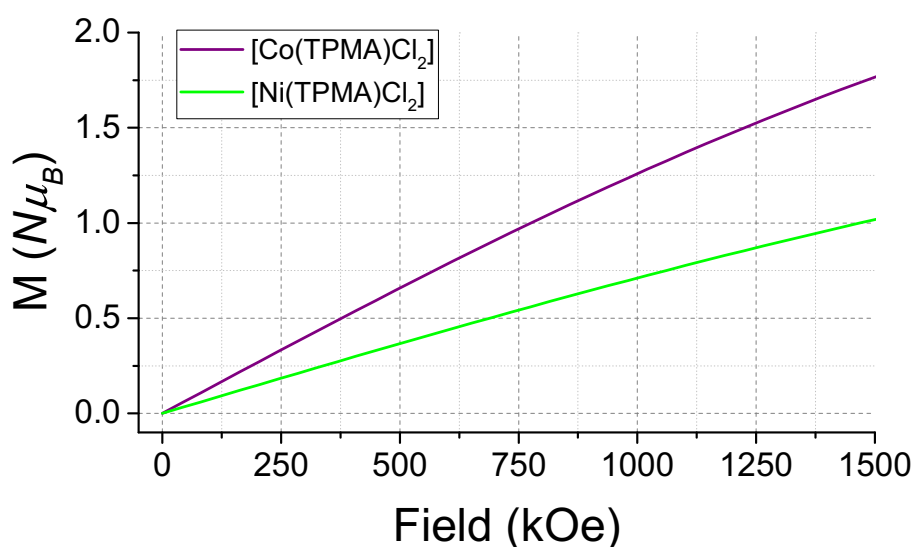
Figure S13. Room temperature simulated magnetization curves for the complexes [Co(TPMA)Cl₂] and [Ni(TPMA)Cl₂], using PHI.[1] The parameters used for the simulation of the M v. H curves have been determined fitting the magnetic data for the complexes. 2500 Oe DC magnetic susceptibility and 2-10 K magnetization curves were measured for each complex. Polycrystalline samples of the latter were constrained in pressed parafilm and placed in gel capsule. Data were corrected for the sample holder and sample diamagnetic contributions. Using PHI[1], the best simultaneous fit of all data for each complex gave the parameters used above and are the following: g_{iso} = 2.06, λ = -96 cm^{-1}, α = 1.35, Δ = 521 cm^{-1}, for [Co(TPMA)Cl₂]; g_{iso} = 2.22, D = -5.1 cm^{-1}, E = 0.3 cm^{-1} for [Ni(TPMA)Cl₂].
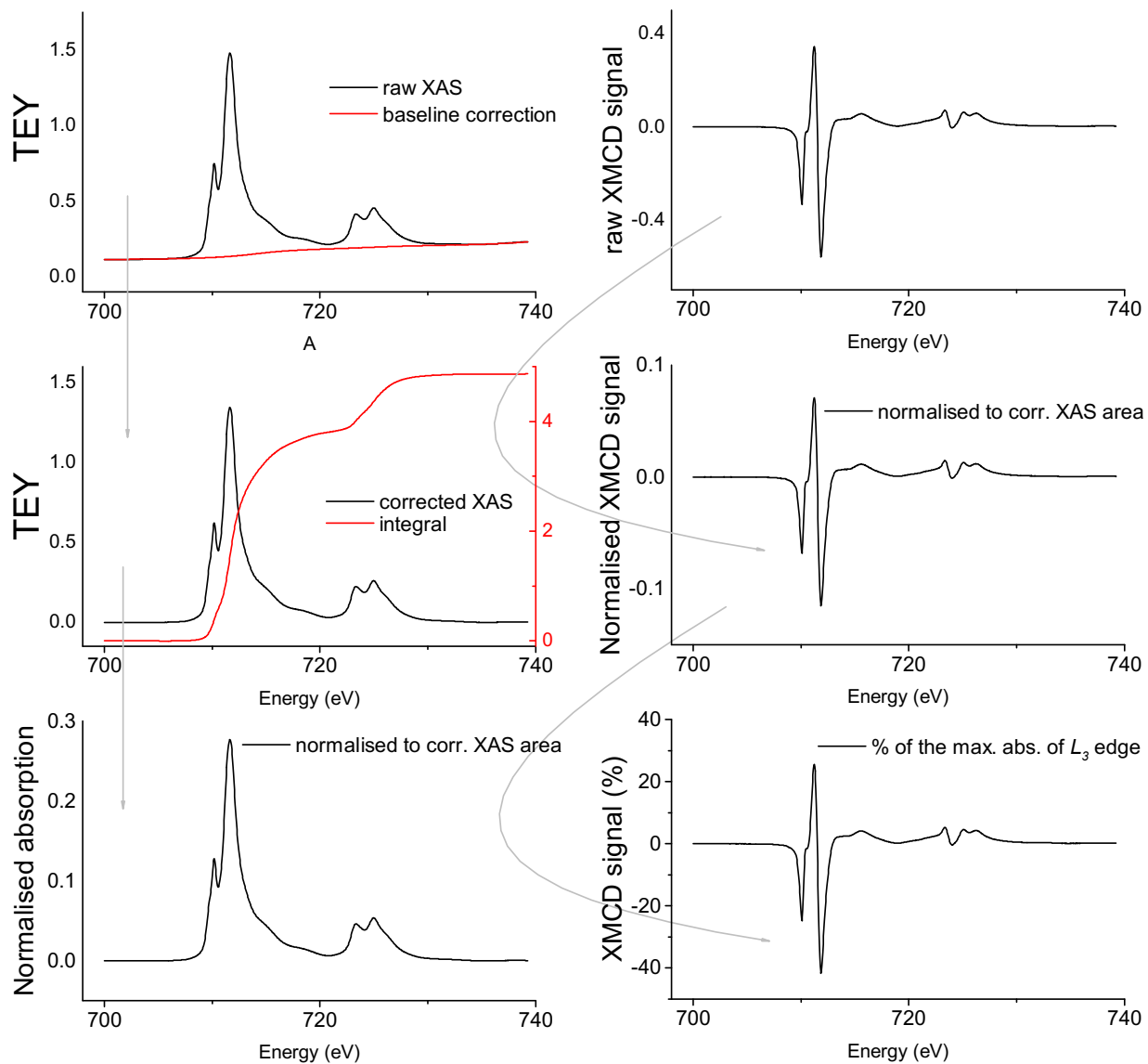
Figure S14. Graphical representation of the different steps for the normalization of the Fe $L_{2,3}$ edges XAS spectra and XMCD signals in γ-Fe$_2$O$_3$, γ-Fe$_2$O$_3$@{Co(TPMA)} and γ-Fe$_2$O$_3$@{Ni(TPMA)}.
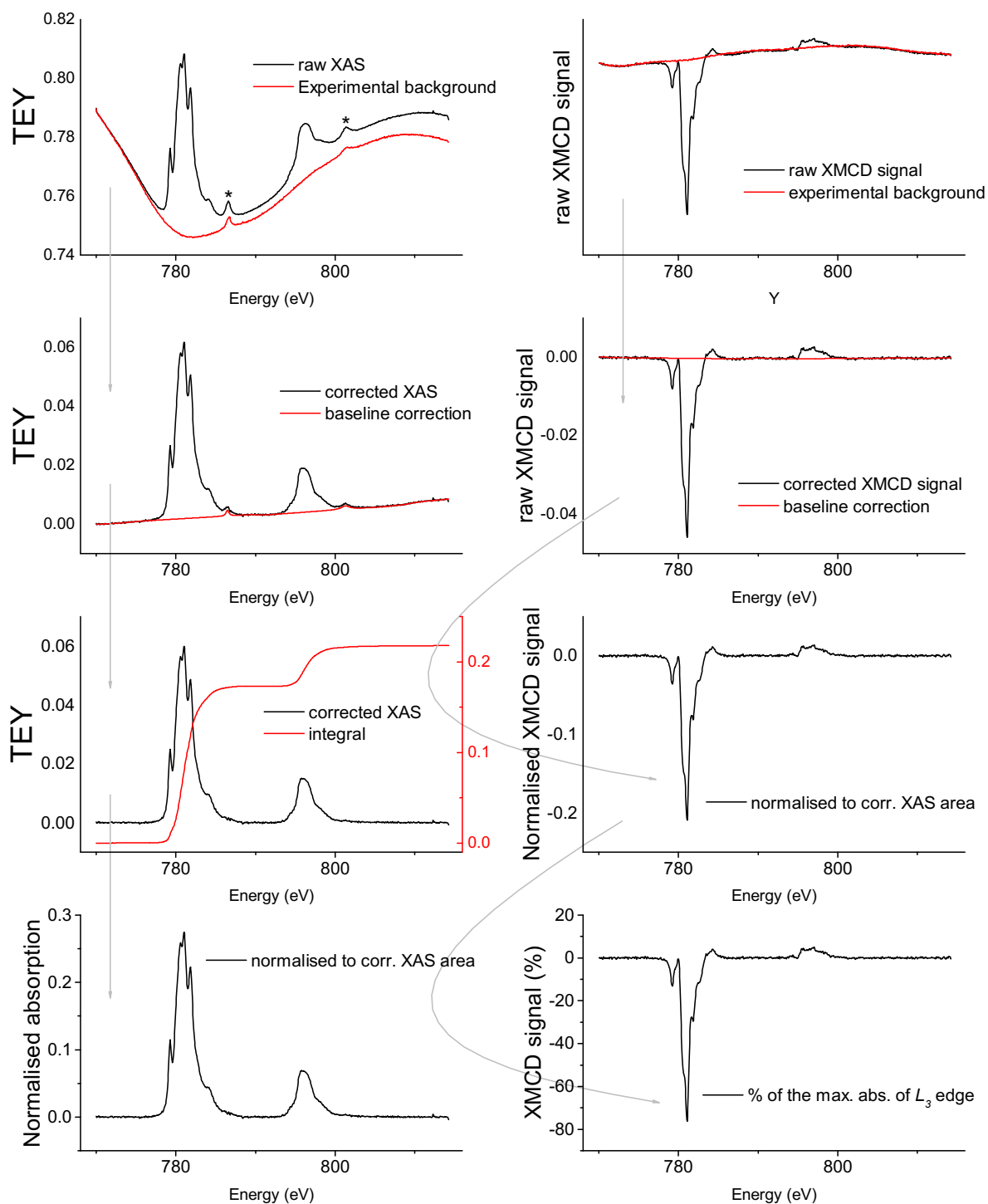
Figure S15. Graphical representation of the different steps for the normalization of the Co $L_{2,3}$ edges XAS spectra and XMCD signals in γ-Fe$_2$O$_3$@{Co(TPMA)}. The same method was used for γ-Fe$_2$O$_3$@{Ni(TPMA)}. Asterisks indicate the $M_{4,5}$ edges absorption peaks coming from trace amounts of Ba in the Si wafer.

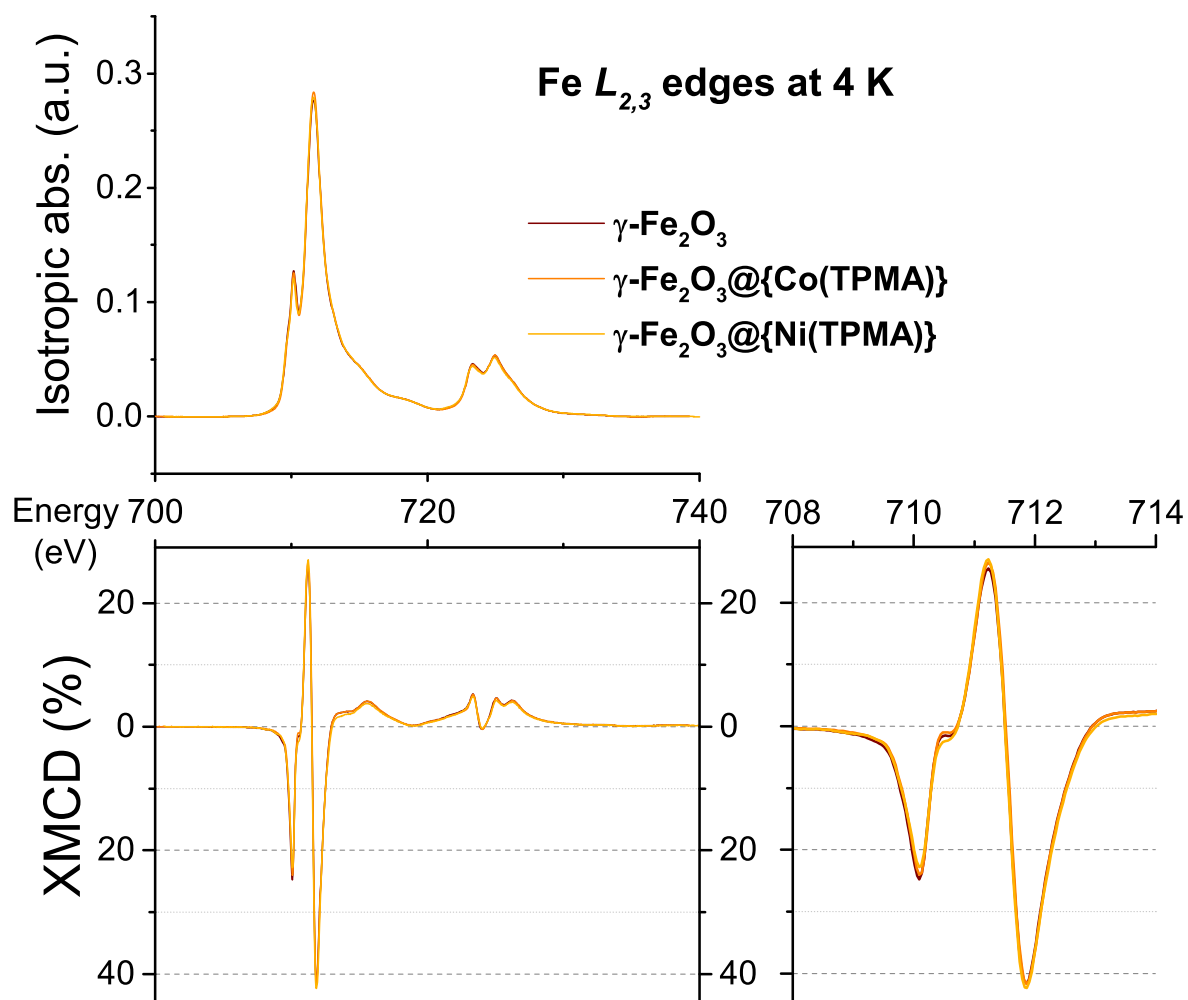**Figure S16**. Comparison of the Fe $L_{2,3}$ edges measured at 4 K and ± 60 kOe in γ-Fe₂O₃, γ-Fe₂O₃@{Co(TPMA)} and γ-Fe₂O₃@{Ni(TPMA)}.
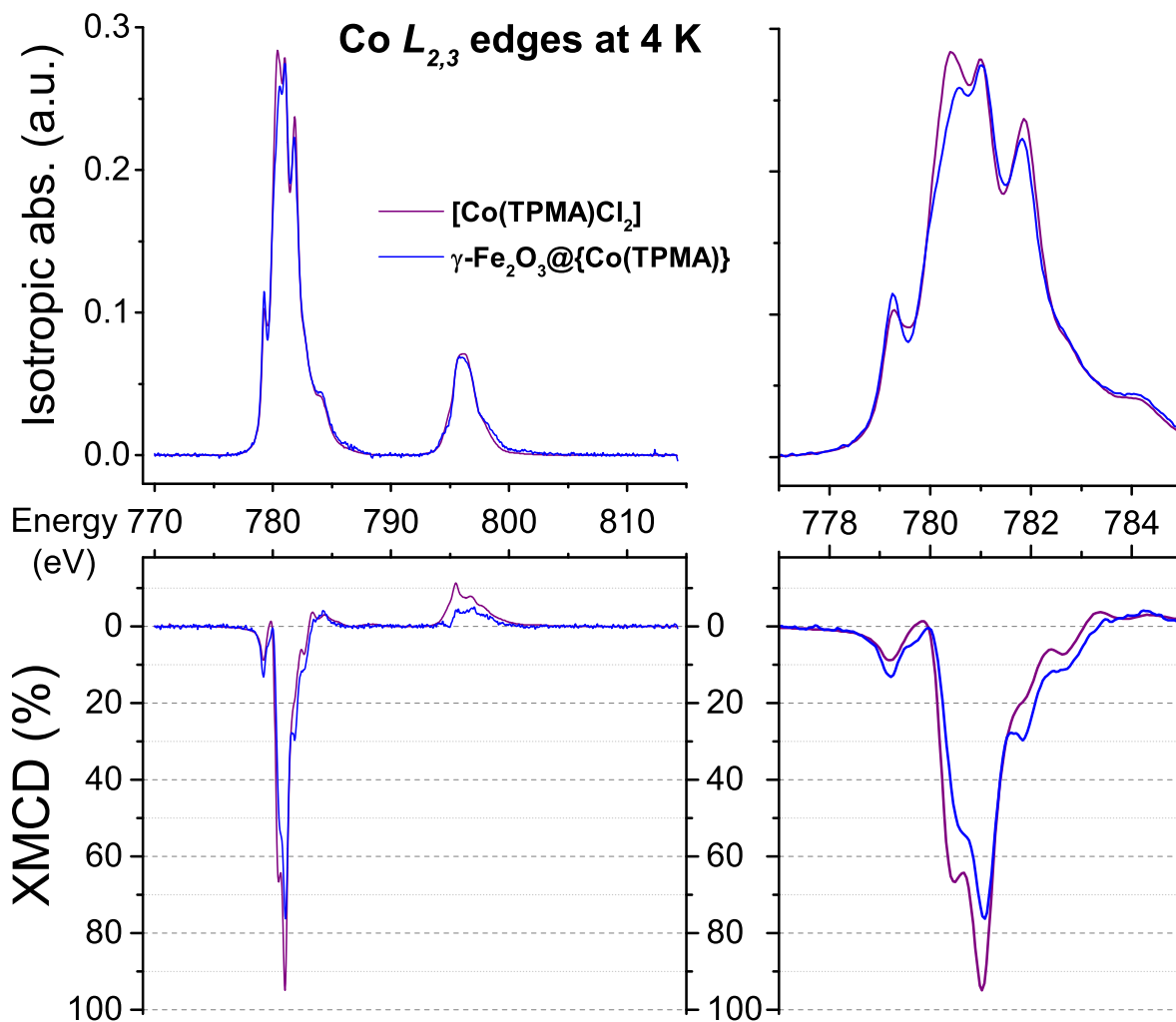
Figure S17. Comparison of the Co $L_{2,3}$ edges measured at 4 K and ± 60 kOe in γ-Fe₂O₃@{Co(TPMA)} and [Co(TPAM)Cl₂].
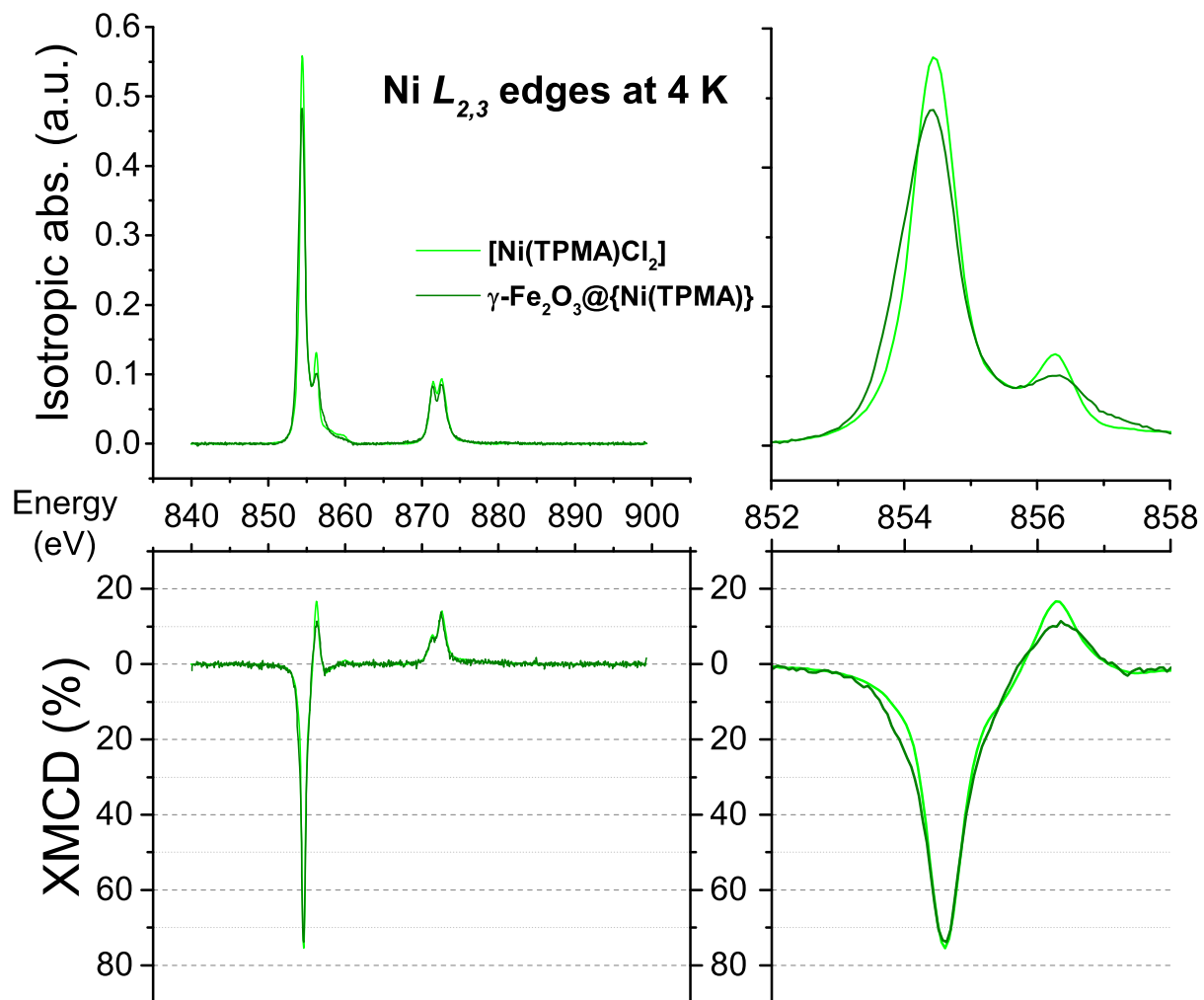
Figure S18. Comparison of the Ni $L_{2,3}$ edges measured at 4 K and ± 60 kOe in γ-Fe₂O₃@{Ni(TPMA)} and [Ni(TPAM)Cl₂].

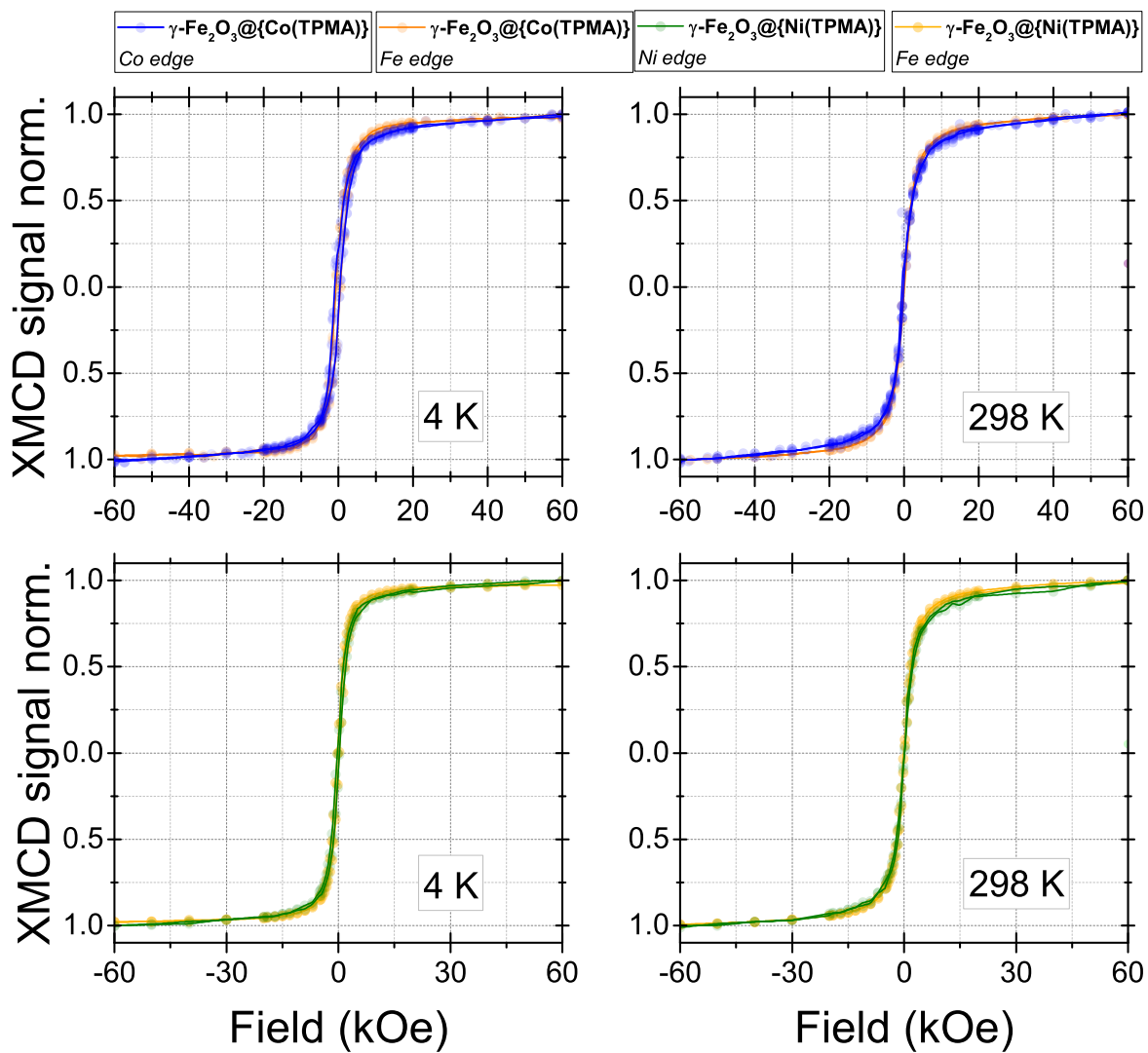**Figure S19.** Field-dependence of the *Oh* Fe L_3, Co L_3 and Ni L_3 edges normalized XMCD signals for γ-Fe₂O₃@{Co(TPMA)} and γ-Fe₂O₃@{Ni(TPMA)} at 4 K and 298 K.
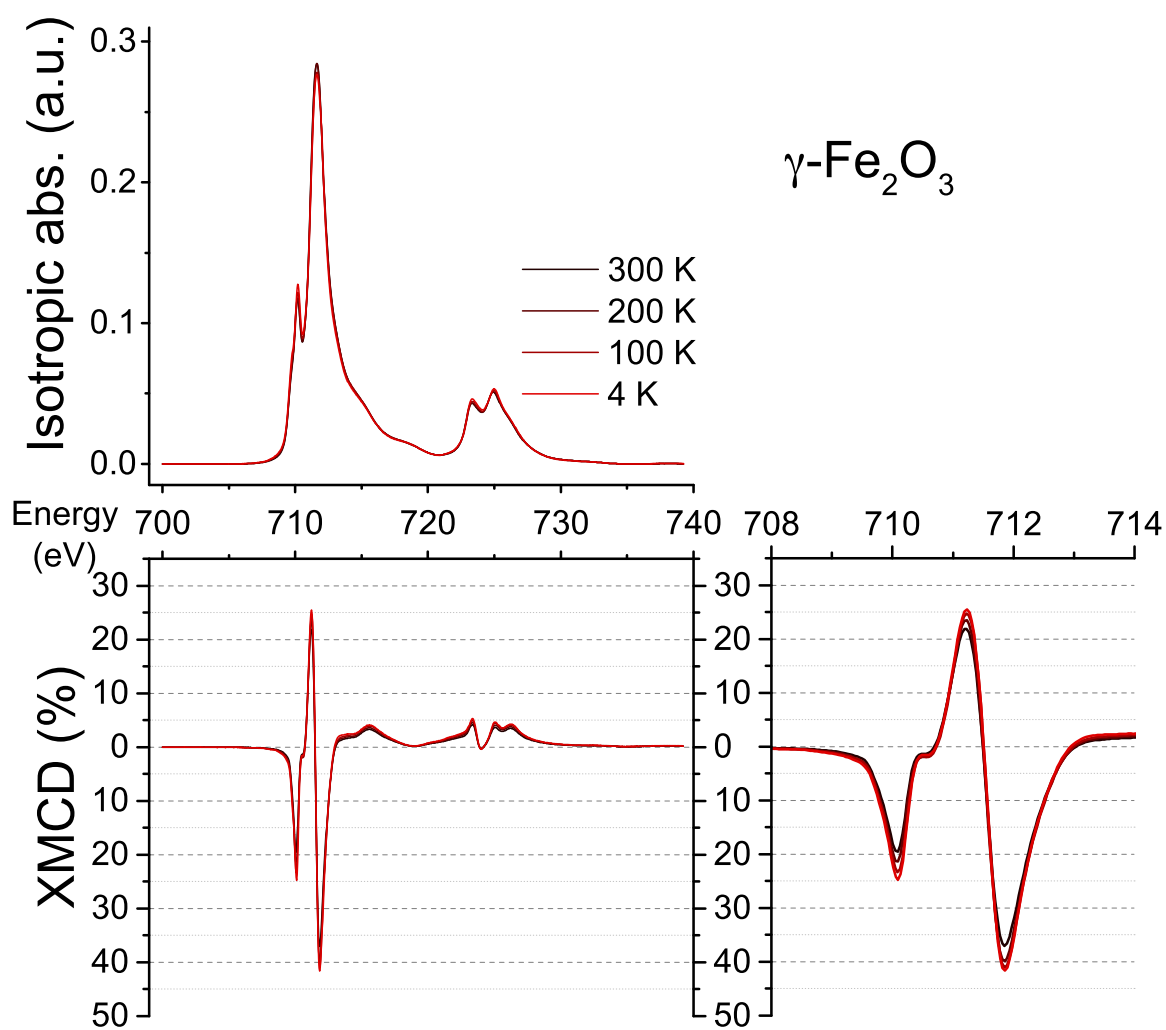
Figure S20. Temperature-dependence of the XAS spectra and XMCD signals in **γ-Fe₂O₃**, from 5 to 300 K at ± 60 kOe.

Figure S21. Temperature-dependence of the XAS spectra and XMCD signals in γ-Fe₂O₃@{Co(TPMA)}, from 5 to 300 K at ± 60 kOe.
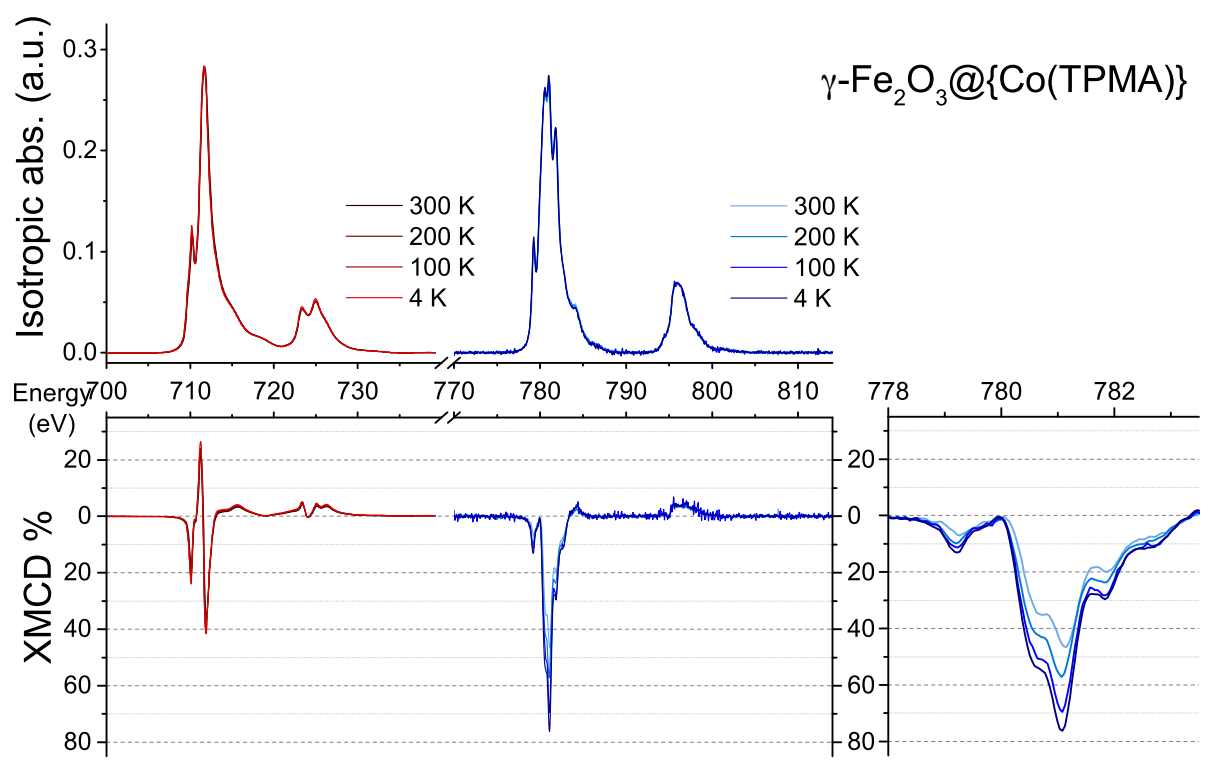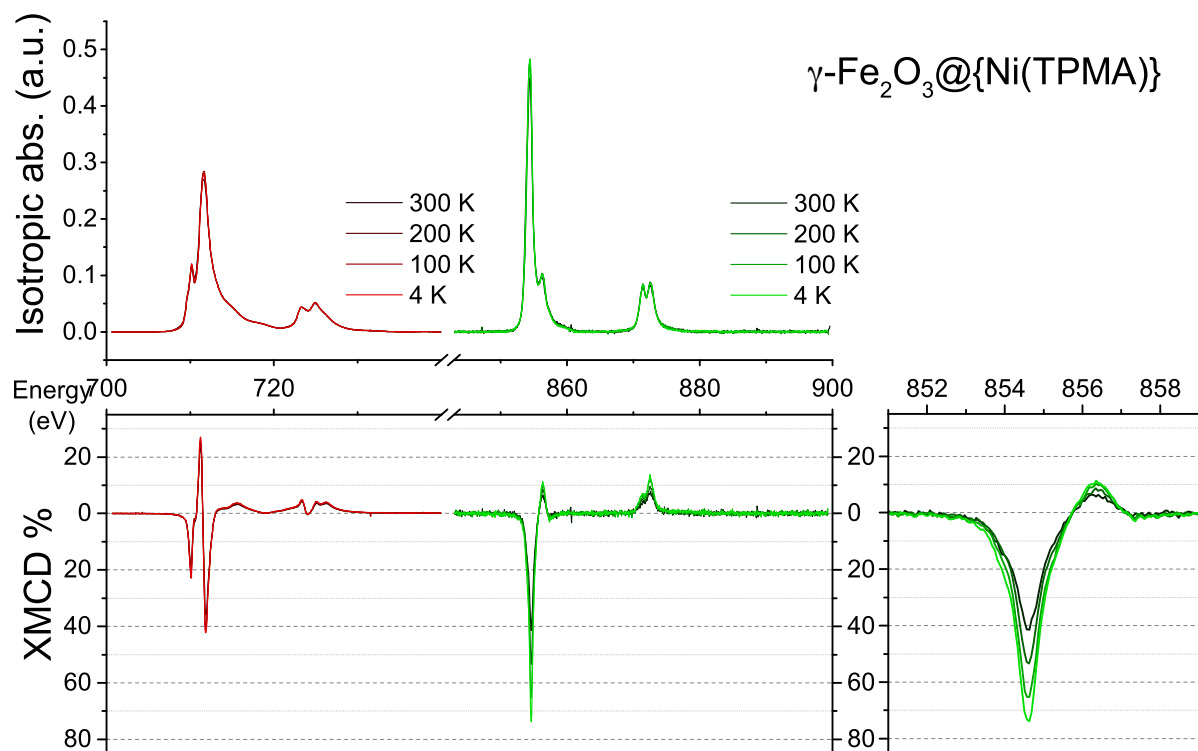
Figure S22. Temperature-dependence of the XAS spectra and XMCD signals in γ-Fe₂O₃@{Ni(TPMA)}, from 5 to 300 K at ± 60 kOe.
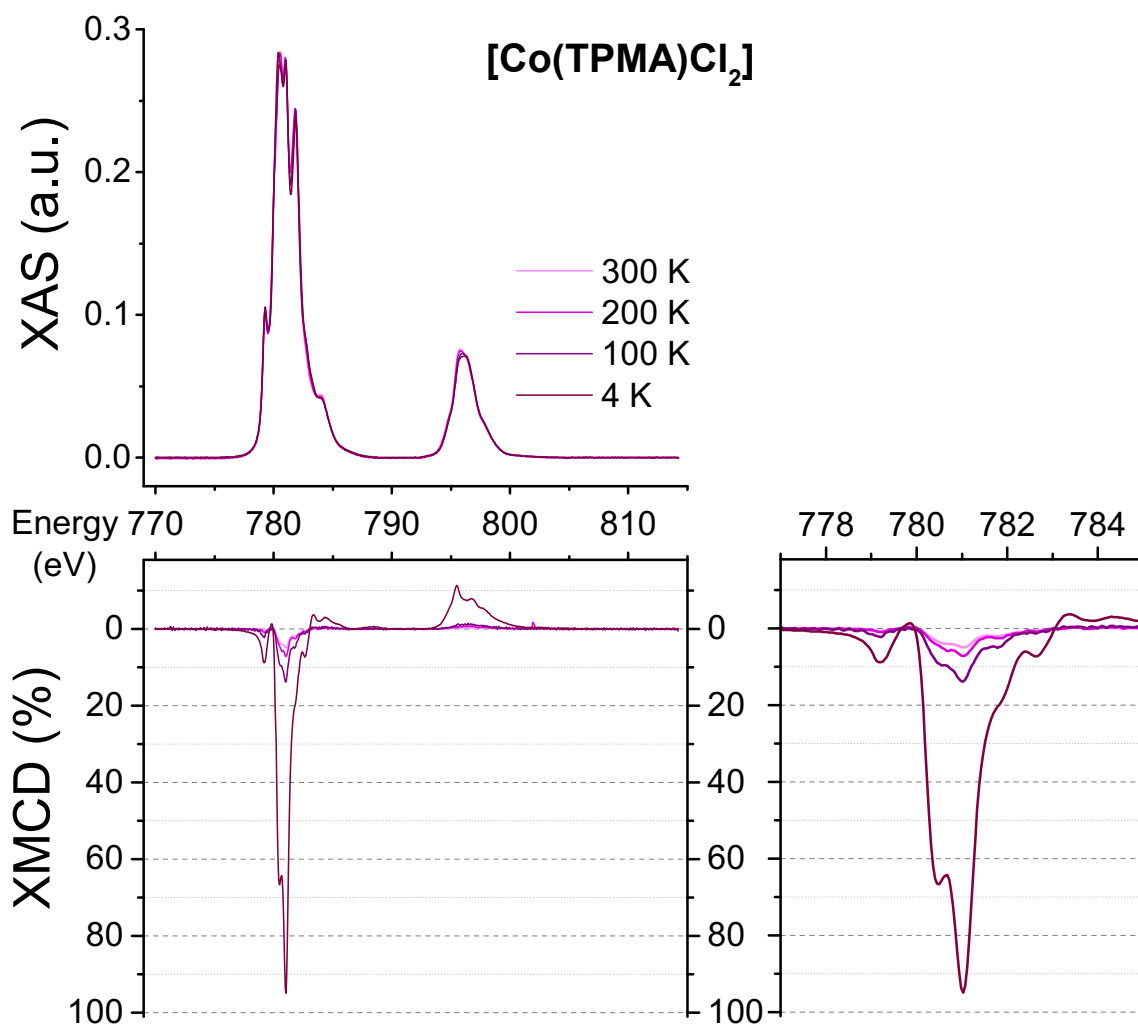
Figure S23. Temperature-dependence of the XAS spectra and XMCD signals in [Co(TPAM)Cl₂], from 5 to 300 K at ± 60 kOe.

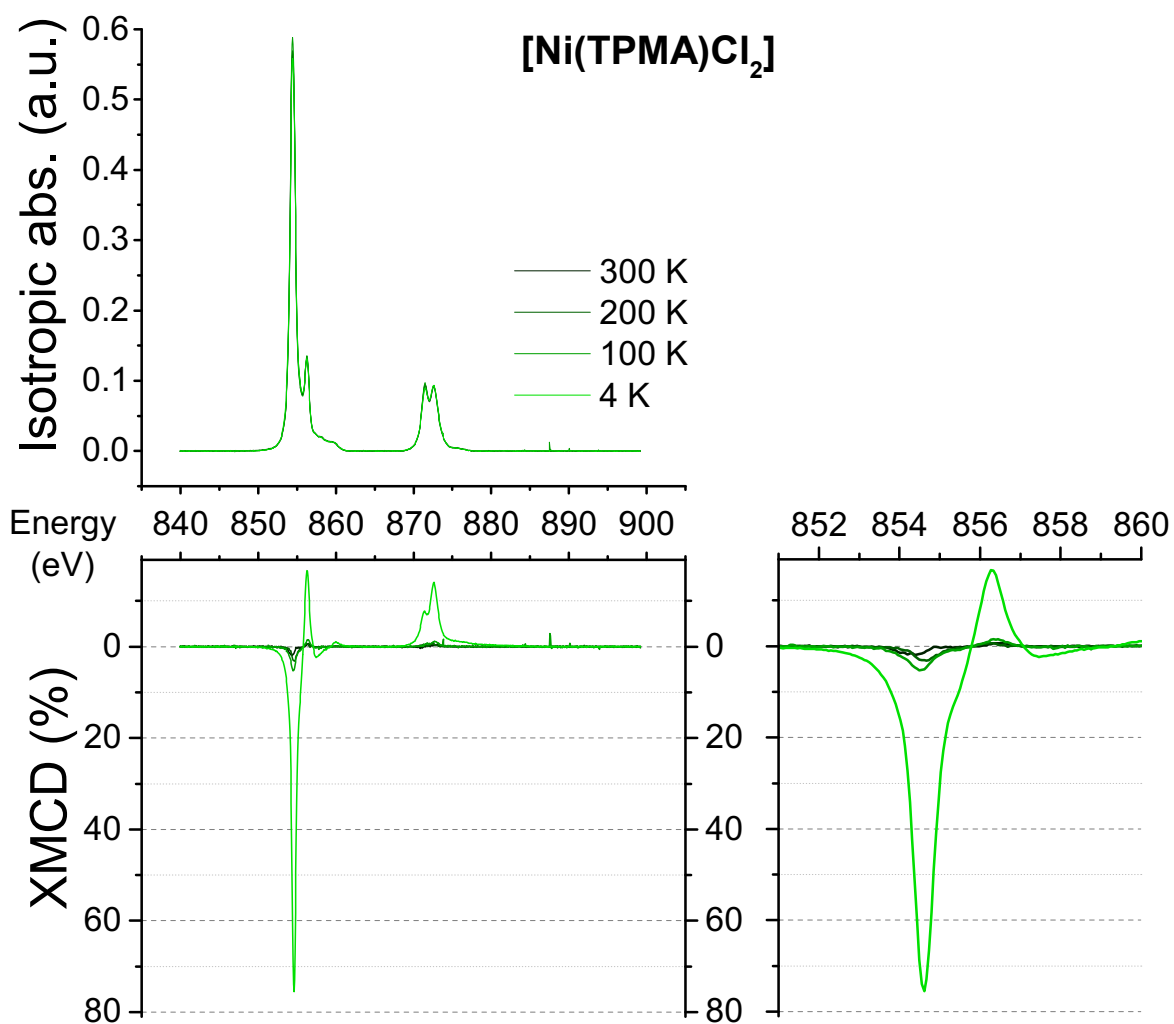**Figure S24.** Temperature-dependence of the XAS spectra and XMCD signals in [Ni(TPAM)Cl₂], from 5 to 300 K at ± 60 kOe.
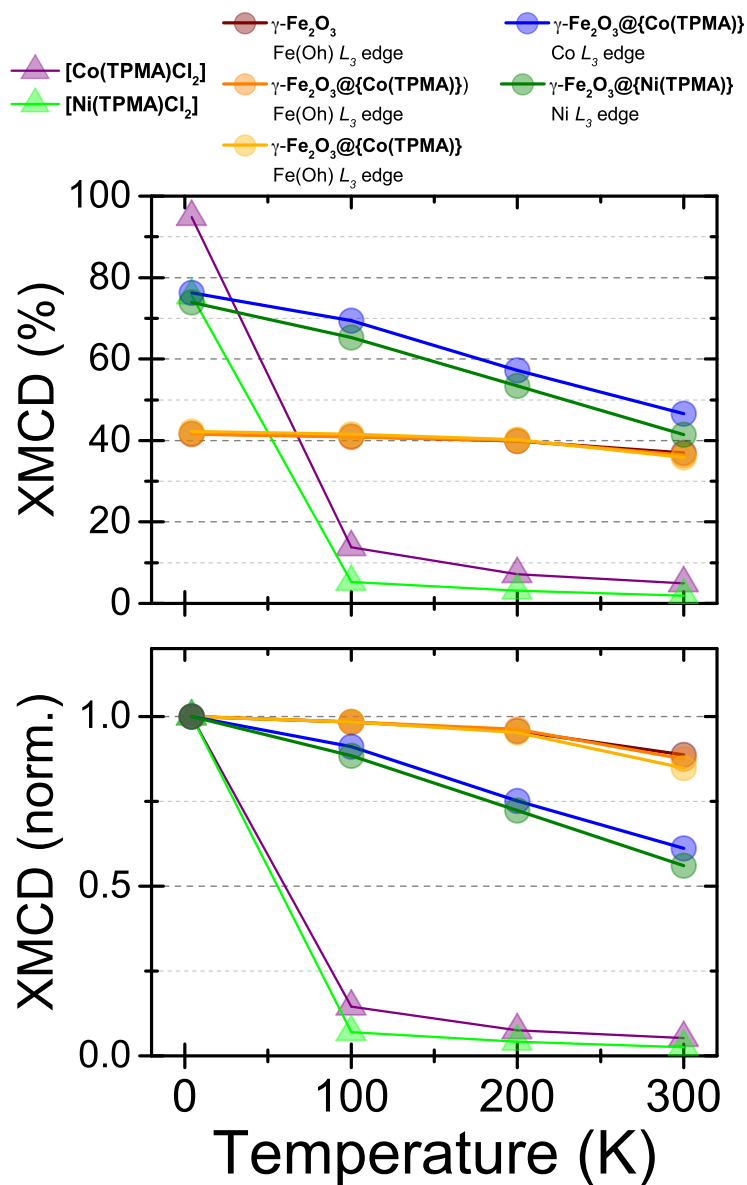
Figure S25. Temperature-dependence of the intensity of the XMCD signals (in % of the XAS maxima at the top, normalized to 1 at the bottom) at the *Oh* Fe(III), Co and Ni *L₃* edge for **γ-Fe₂O₃**, **γ-Fe₂O₃@{Co(TPMA)}**, **γ-Fe₂O₃@{Ni(TPMA)}**, [Co(TPMA)Cl₂] and [Ni(TPMA)Cl₂],
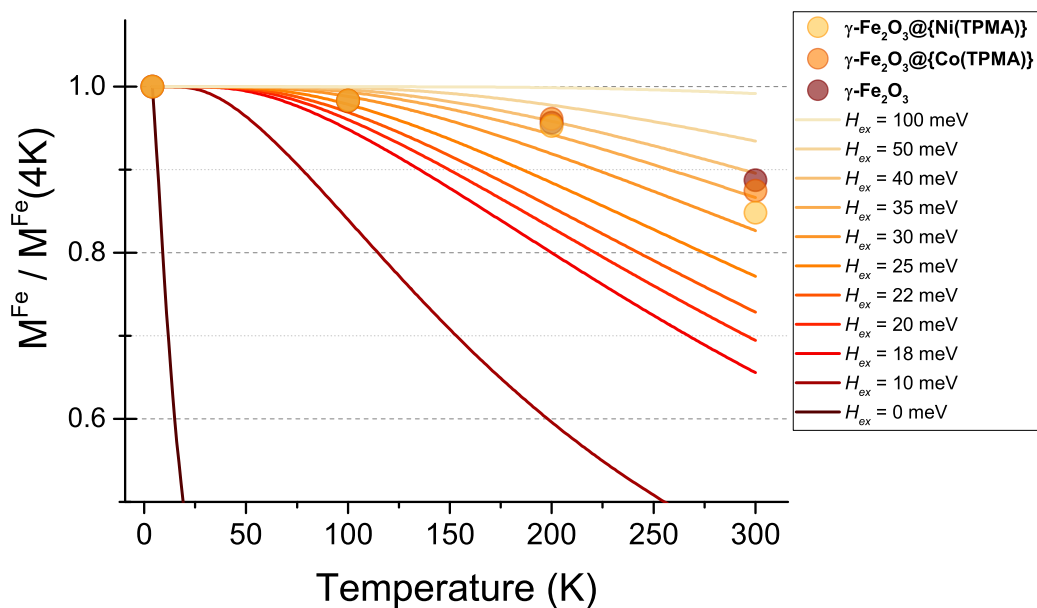
Figure S26. Simulation of *M(T)/M(4K)* for different exchange field values together with the normalized experimental *Oh* Fe(III) XMCD values for **γ-Fe₂O₃**, **γ-Fe₂O₃@{Co(TPMA)}**, and **γ-Fe₂O₃@{Ni(TPMA)}**. The magnetic moments were calculated within the Ligand Field Multiplet theory with the Quanty code.[2–4] The eigenstates of Fe(II) were calculated using *Oh* symmetry and a fixed H_{ex} value, within an external 60 kOe magnetic field. A ligand field strength of $10Dq$ = 1 eV was used. The magnetic moments were calculated at each temperature using the Boltzmann distribution.

Estimation of the number of iron(III) ions (n) influenced by the Co(II) complexes:

$$n_{Fe}^{tot} = 4908$$

γ-Fe$_2$O$_3$: 1

γ-Fe$_2$O$_3$@{Co(TPMA)} : 2

$$H_{C_{Fe}}^{\mathbf{1}} = 270\ Oe;\ H_{C_{Fe}}^{\mathbf{2}} = 590\ Oe; H_{C_{Co}}^{\mathbf{2}} = 710\ Oe$$

$$H_{C_{Fe}}^{\mathbf{2}} = \frac{(n_{Fe}^{tot} - n) \times H_{C_{Fe}}^{\mathbf{1}} + n \times H_{C_{Co}}^{\mathbf{2}}}{n_{Fe}^{tot}}$$

$$n = \frac{n_{Fe}^{tot} \times (H_{C_{Fe}}^{\mathbf{2}} - H_{C_{Fe}}^{\mathbf{1}})}{H_{C_{Co}}^{\mathbf{2}} - H_{C_{Fe}}^{\mathbf{1}}} = 3570$$

1 N. F. Chilton, R. P. Anderson, L. D. Turner, A. Soncini and K. S. Murray, *J. Comput. Chem.*, 2013, 34, 1164–1175.
2 Quanty - a quantum many body script language - Quanty, https://quanty.org/, (accessed February 8, 2024).
3 M. W. Haverkort, M. Zwierzycki and O. K. Andersen, *Phys. Rev. B*, 2012, 85, 165113.
4 M. W. Haverkort, *J. Phys.: Conf. Ser.*, 2016, 712, 012001.